

Journal of Materials Chemistry A

Accepted Manuscript



This is an *Accepted Manuscript*, which has been through the Royal Society of Chemistry peer review process and has been accepted for publication.

Accepted Manuscripts are published online shortly after acceptance, before technical editing, formatting and proof reading. Using this free service, authors can make their results available to the community, in citable form, before we publish the edited article. We will replace this *Accepted Manuscript* with the edited and formatted *Advance Article* as soon as it is available.

You can find more information about *Accepted Manuscripts* in the [Information for Authors](#).

Please note that technical editing may introduce minor changes to the text and/or graphics, which may alter content. The journal's standard [Terms & Conditions](#) and the [Ethical guidelines](#) still apply. In no event shall the Royal Society of Chemistry be held responsible for any errors or omissions in this *Accepted Manuscript* or any consequences arising from the use of any information it contains.

Cite this: DOI: 10.1039/c0xx00000x

ARTICLE TYPE

www.rsc.org/xxxxxx

Enhanced selective CO₂ adsorption on polyamine/MIL-101(Cr) composites

Yichao Lin,^a Hao Lin,^{a,b} Haimin Wang,^b Yange Suo^a, Baihai Li,^a Chunlong Kong^{*a} and Liang Chen^{*a}*Received (in XXX, XXX) Xth XXXXXXXXX 20XX, Accepted Xth XXXXXXXXX 20XX*

DOI: 10.1039/b000000x

The global climate change induced by greenhouse gases has stimulated active research for developing efficient strategies to mitigate CO₂ emission. In the present study, we prepared a series of polyamine/metal-organic frameworks (MOF) composites as highly selective CO₂ adsorbents from CO₂/N₂ mixture, which is relevant to CO₂ capture in the flue gas. We show that loading polyethyleneimine (PEI) into MIL-101(Cr) frameworks can significantly enhance the selective CO₂ adsorption capacity at low pressure and ambient temperature. Further, the comparative study reveals that both the particle size of MOF and molecular-weight of PEI play an important role in the CO₂ capture ability. Regarding the particle size, smaller MIL-101(Cr) particles can facilitate the loading of PEI into the inner pores and result in lower surface area/pore volume. Thus, the resulting PEI/MIL-101(Cr) composites possess relatively lower CO₂ adsorption capacity, but are compensated by higher selectivity of CO₂ over N₂. On the other hand, lower molecular-weight linear PEI could readily diffuse into the inner pores and effectively block the N₂ adsorption. As a result, the as-prepared A-PEI-300 sample in this work exhibits an excellent CO₂ uptakes of 3.6 mmol·g⁻¹ and ultrahigh CO₂/N₂ selectivity at 0.15 bar and 25 °C. In contrast, the higher molecular-weight branched PEI is advantageous at elevated temperature, since the composites can retain high CO₂ adsorption capacity owing to the large amount of primary amine groups. Overall, polyamine/MOF composites are shown to be good candidate adsorbents for CO₂ capture from flue gas. To achieve the optimal CO₂ capture ability, a comprehensive optimization of the polyamine and MOF structures should be performed.

Introduction

The rapidly increasing concentration of carbon dioxide (CO₂) in atmosphere, which mainly stems from the combustion of fossil fuels, has become a major environmental concern.¹ The efficient separation and sorption of CO₂ from flue gas, especially at low pressure and ambient temperature, is a key step in the carbon capture and sequestration process. Currently, amine-based solutions are widely used in large scale to capture CO₂ from industrial streams because they have high CO₂ absorption capacity. However, the high heat capacity of these solutions makes the regeneration very energy intensive.² Instead, amine-functionalized solid adsorbents are emerging as more promising candidates for CO₂ capture because the heat capacity of solids are much lower. Furthermore, the corrosion and volatility³ issues intrinsic to amine solutions, could be significantly minimized in solid adsorbents. For example, amine-incorporated zeolite and silica adsorbents have been successfully prepared with excellent selective CO₂ adsorption capacity recently.⁴⁻¹³ Based on these studies, it is concluded that both the porosity of solid adsorbents and the amount of amine loaded determine their CO₂ adsorption capacity.⁵ In particular, the porosity of solid acceptor is the key factor. Thus, porous materials with high porosity and suitable pore size are highly demanded for developing amine-functionalized adsorbents with high CO₂ capture capacity.

In the last two decades, a large number of metal-organic frameworks (MOFs), have been successfully synthesized.¹⁴⁻¹⁹ Among the numerous attractive traits of this new family of solid porous materials are their well-characterized crystalline architectures, ultrahigh porosity and the possibility of functionality. Hence, they have been extensively investigated for the potential application in gas storage and gas separation.²⁰⁻²³ However, very limited MOFs can display satisfactory CO₂ capture performance at low pressure and ambient temperature due to the weak interaction between CO₂ and frameworks, albeit some MOFs^{24,25} have been reported with excellent CO₂ adsorption capacity. Moreover, covalent grafting of amine groups to the aromatic rings in MOFs cannot significantly enhance their CO₂ capture performance because of the electron withdrawing effect of benzene ring.²⁶⁻²⁹

Indeed, some recent studies show that diamine and polyamine incorporated into the framework of MOFs, can dramatically enhance the selective CO₂ adsorption capacity at low pressure and ambient temperature.³⁰⁻³² The MOF/polyamine composites display high CO₂ capture capacity because the dispersed polyamine in MOF framework allowing CO₂ molecules diffusion and adsorption, whereas the pure polyamine commonly becomes gel, which hinders the diffusion of CO₂ molecules and interaction with amine groups.³³ MOF mainly acts as the support for loading polyamines, while the dispersed polyamines directly determine the adsorption capacity and selectivity of CO₂.

In a previous study, we chose linear polyethyleneimine (PEI, with an average molecular-weight of 300) and MIL-101(Cr) as the model system to fabricate PEI-incorporated MOF adsorbents.^{30,32} MIL-101(Cr) is chosen because of its high porosity, excellent thermal and chemical stability, as well as high resistance to moisture. Furthermore, the open metal sites in MIL-101(Cr) could anchor amine groups of the PEI to form stable PEI/MIL-101(Cr) composites. The resulting composite exhibit a very competitive CO₂ adsorption capacity of 4.2 mmol.g⁻¹ at 25 °C and 0.15 bar, as well as excellent selectivity for CO₂ over N₂ in the designed flue gas with 0.15 bar CO₂ and 0.75 bar N₂. On the basis of this study, we conceive and evaluate two strategies to further improve the CO₂ adsorption capacity and selectivity in the present study: (1) Shrink the MOF crystal size as the smaller MOF particles are expected to facilitate the loading of PEI into the pores. Hence, we comparatively investigate MIL-101(Cr) crystals with around 150 nm (denoted as A hereafter) and 250 nm (B). Both of them have high BET surface area (> 3000 m².g⁻¹). Note that, to further shrink the particle size down to less than 100 nm, the surface area is dramatically decreased to around 2000 m².g⁻¹, accompanied by a very poor crystallinity. Thus, we did not choose them for loading PEI. (2) Load branched PEI into the MIL-101(Cr) pores. As shown in Figure 1, we anticipate that the branched PEI with higher molecular-weight possesses abundant primary amine groups (-NH₂) that could display stronger affinity³⁴ for CO₂ than secondary amine groups (-NH-) in the linear PEI used in our previous study. In this work, three PEI with average molecular-weight of 300, 1800 and 10000 are used and the resulting PEI/MIL-101(Cr) composites are denoted as A-PEI-300, B-PEI-300, A-PEI-1800 and A-PEI-10000, respectively. The CO₂ and N₂ adsorption properties, CO₂/N₂ selectivity of all as-prepared adsorbents are evaluated at 25 °C and 50 °C. We will show that all the PEI/MIL-101 adsorbents display much higher selective CO₂ adsorption capacity than MIL-101(Cr). Compared to the previous study, shrinking the MOF crystal size can substantially improve the CO₂/N₂ selectivity, while loading branched PEI can improve the CO₂ adsorption capacity at elevated temperature.

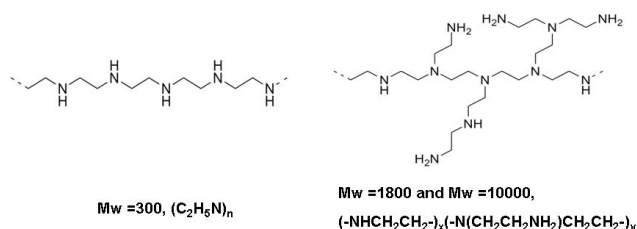


Figure 1. Chemical structures of PEI with average molecular-weight of 300, 1800 and 10000.

Experimental

Materials

1,4-benzene di-carboxylic acid (H₂BDC, Sigma-Aldrich), chromium nitrate [Cr(NO₃)₃·9H₂O, TCI], hydrofluoric acid (HF, Merck), ethanol (EtOH, TCI), lithium acetate (CH₃COOLi, TCI) were used as received from vendors without further purification. Deionized water and alcohol was employed as solvent. Branched polyethyleneimine (M_w=1800 and 10000 Da) and linear

polyethyleneimine (M_w=300Da) in the present study were purchased from Alfa Aesar. Due to the hygroscopic property, PEI was placed in glove box.

Synthesis of MIL-101(Cr) nanoparticles

To obtain the uniform and well-crystallized MIL-101(Cr) crystals, the acetate-assisted hydrothermal synthesis approach was adopted. The detailed process was as follows. First, 1,4-benzene di-carboxylic acid (H₂BDC) (664 mg, 4 mmol), Cr(NO₃)₃·9H₂O (1600 mg, 4 mmol) and a certain amount of acetate were dissolved in distilled water (25 ml, 1389 mmol). Here two different molar ratios of CH₃COOLi/Cr(NO₃)₃ including 0.06:1 and 0.3:1 were used. Second, the mixed reactants were well-dispersed under ultrasonic condition for 30 min, and then heated in a Teflon-lined autoclave at 200 °C for 12 hours under autogenous pressure. The yielded solid was doubly filtered by filter paper and sufficiently washed with distilled water and followed by centrifugation. Finally, the resulting precipitate was transferred to a Teflon-lined autoclave, washed twice by hot ethanol at 90 °C for 4 hours. The obtained product was dried under vacuum at 150 °C overnight.

Synthesis of PEI/MIL-101(Cr) composites

The MIL-101(Cr)-PEI adsorbent was prepared by wet impregnation method. The detailed process was as follows. First, before the impregnation, the MIL-101 (Cr) powders were heated at 160 °C under vacuum condition for 12 h, removing the adsorbed water and coordinated water molecules. Second, a series of 0.2g PEI (M_w=300, 1800 and 10000) was dissolved in 1 mL anhydrous methanol under stirring for 10 min, and then 0.2 g MIL-101 (Cr) powders were added step by step into the PEI/methanol solution under stirring. Finally, the resulting gel was dried overnight at room temperature and under nitrogen protection. The temperature of the sample was increased at programmed rate and held at 110 °C for 12 h under vacuum condition. After that, a porous and solid MIL-101 (Cr)-PEI adsorbent was obtained. Herein, four MIL-101 (Cr)-PEI samples with same PEI loadings were prepared, corresponding to A-PEI-300, A-PEI-1800, A-PEI-10000 and B-PEI-300. To confirm the accurate PEI loading, the mass of MIL-101(Cr) was measured immediately after activated, and the mass of PEI was measured in glove box.

Characterizations

Powder XRD data of the product was collected on a Bruker AXS D8 Advance diffractometer using CuKα radiation at room temperature. The powder XRD was scanned over the angular range of 5-30° (2θ) with a step size of 0.02° (2θ). IR of the samples were recorded on KBr/sample pellets in a Thermo model Nicolet 6700 spectrometer to determine the amine. IR spectra were collected on activated MIL-101 (Cr)-PEI and MIL-101 (Cr) samples under vacuum condition. IR spectra of pure PEI are also shown for comparison. The as-prepared crystal morphology was examined using a Field Emission Scanning Electron Microscope (Hitachi, S-4800). The nitrogen adsorption/desorption isotherm was measured on ASAP 2020M apparatus. The BET surface area was calculated over the range of relative pressures between 0.05 and 0.20 bar. Before measurement, the sample was outgassed under vacuum at 110 °C for 12 h. Thermogravimetric analysis (TGA) was measured using a system provided by Mettler Toledo (model TGA/DSC1), in air at a heating rate of 10 °C/min up to 600 °C. Before the TGA measurement, the samples were first activated and then placed in atmosphere for the same time (one week).

Adsorption

The PEI/MIL-101(Cr) composites were immediately measured after moving from the glove box. The adsorption kinetics of CO₂ was measured using volumetric technique by the apparatus from SETARAM France (PCTpro-E&E). Before each measurement, the sample was evacuated at 110 °C for 12 h. In the adsorption measurement, the apparatus first gave a desired pressure CO₂ gas to the sample holder, and we recorded the pressure values in the sample holder and calculated the amount of adsorbed CO₂.

The adsorption isotherms of CO₂ and N₂ were measured using volumetric technique by an apparatus from SETARAM France (PCTpro-E&E). The amount of CO₂ adsorbed as a function of pressure was determined using the Langmuir-Freundlich³⁵⁻³⁸ fit for the isotherms:

$$\frac{Q}{Q_m} = \frac{B \times P^{(1/t)}}{1 + B \times P^{(1/t)}}$$

Here, Q and Q_m are the uptake and the maximum uptake, respectively. p is the equilibrium pressure, B and t are the equation constants. To obtain the exact pressures p, corresponding to constant amount of CO₂ adsorbed, the above equation can be rearranged to:

$$P = \left(\frac{Q/Q_m}{B - B \times Q/Q_m} \right)^t$$

The CO₂/N₂ adsorption selectivities (α) of all samples were calculated by the following equation, according to a previous report^{32,39}:

$$\alpha = \frac{Q_{CO_2}/P_{CO_2}}{Q_{N_2}/P_{N_2}}$$

where Q_i is the adsorption capacity of component i, P_i is the partial pressure of component i. The adsorption capacities of the components are defined as the molar excess adsorption capacities determined without correction for absolute adsorption.

In the experiment of adsorption property influenced by water vapor, the B-PEI-300 sample was first activated under 110 °C under vacuum condition for 12 hours. Then, the mass was immediately measured (m₁), after that the B-PEI-300 sample was quickly transferred to a vacuum box, together with a cup of deionized water. The vacuum box was then evacuated and heated at 80 °C. Two hours later, the sample was quickly transferred to an apparatus sample holder for CO₂ adsorption measurement.

The regeneration ability index of CO₂ adsorption capability under different desorption temperature were also measured using volumetric technique by the apparatus from SETARAM France (PCTpro-E&E). The fresh sample was evacuated at 110 °C for 12 h. At other desorption temperature, the samples were evacuated for 1h.

The breakthrough curve experiments for CO₂/N₂ mixture were carried out using a column with a length of 20 cm and an internal diameter of 0.8 cm. The sample powder was packed in the middle part of the column. Here, the sample mass we used is 0.30 g. Breakthrough allows in situ activation of the sample under argon flow. The detailed experiment methodology can be found in references.^{40,41} The flow rates of all pure gases were controlled by mass flow controllers. Before the measurement, the sample was

activated at 110 °C for 2 h. The gas stream from the column outlet was analyzed online with a mass spectrometer.

Results and Discussion

55 Characterization of PEI/MIL-101 composites

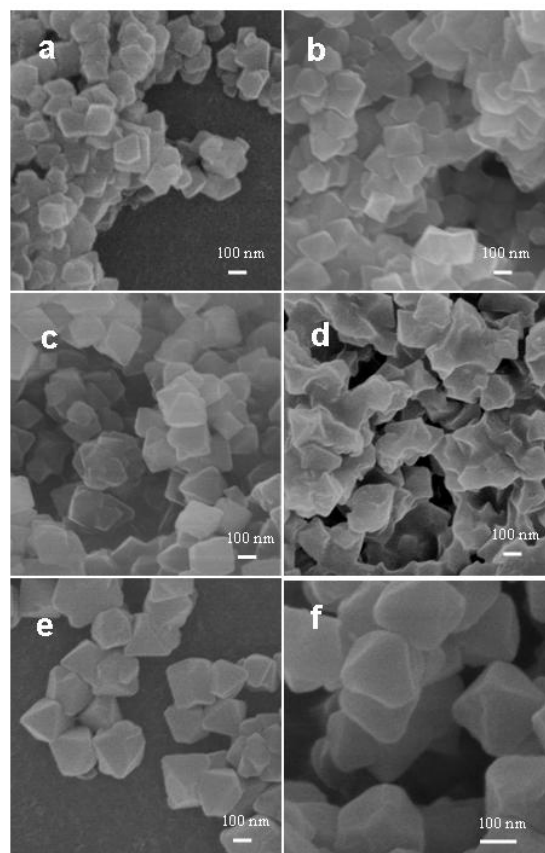


Figure 2. SEM images of A (a), A-PEI-300 (b), A-PEI-1800 (c), A-PEI-10000 (d), B (e) and B-PEI-300 (f).

Scanning electron microscope (SEM), X-ray diffraction (XRD), thermogravimetric analysis (TGA), infrared spectroscopy (IR) and N₂ adsorption/desorption at 77 K are used to characterize the as-prepared PEI-MIL-101(Cr) adsorbents. Clearly, powder XRD patterns of the samples show that the Bragg diffraction angles in MIL-101(Cr) and PEI-incorporated MIL-101(Cr) samples are essentially identical (Figures S1 and S2), indicating that the MIL-101(Cr) structure is well maintained after loading PEI. However, it can be seen that the peaks below 7° of MIL-101(Cr) almost disappear after loading PEI. This is attributed to the filling of MIL-101(Cr) pores of PEI.³² Actually, similar phenomenon has also been observed on PEI-loaded SBA-15 adsorbent.⁵ Note that the intensity of peaks above 7° of A-PEI-1800, A-PEI-10000 and B-PEI-300 remains intact, whereas the intensity of some peaks above 7° of A-PEI-300 is decreased significantly. Apparently, it suggests that linear PEI with small molecular-weight can be more readily loaded into the inner pores of small MIL-101(Cr) particles. In contrast, PEI with large molecular-weight or large MIL-101(Cr) crystals leads to relatively high diffusion resistance of PEI, which is unfavorable for loading PEI into MIL-101(Cr) pores. This is also corroborated by the SEM images. As shown in

Figure 2, the morphologies of MIL-101(Cr) after loading PEI remain nearly intact, except for A-PEI-10000. Apparently, the surface of MIL-101(Cr) crystals is covered with some PEI-10000, indicating that PEI with too large molecular-weight cannot be completely loaded into MIL-101(Cr) framework pores, albeit the crystal size is small.

To ensure that PEI is successfully incorporated into the MIL-101(Cr) framework, IR spectra are collected on activated MIL-101(Cr) and PEI/MIL-101(Cr) samples. As shown in Figure S3, the representative peaks between 3500 cm^{-1} and 2800 cm^{-1} corresponding to -NH and -CH stretching vibrations can be observed on PEI/MIL-101(Cr) samples, which are ascribed to that of pure PEI. TGA measurement is employed to evaluate the thermal stability of the as-prepared samples. As shown in Figure S4, the PEI-incorporated MIL-101(Cr) samples distinctly exhibit the sharp weight loss of PEI at higher temperatures. Furthermore, the decomposition temperature of MIL-101(Cr) is also increased slightly. It implies that the incorporated-PEI should strongly interact with the framework of MIL-101(Cr), most likely on the open Cr sites. In contrast, no elevated decomposition temperature of PEI is found in PEI-loaded silica and zeolite adsorbents.⁴² Here we note that the molecular-weight of PEI has no influence on the thermal stability of resulting composites, albeit the decomposition temperatures of the pure PEI are different.

Table 1. Textural Properties for the synthesis of MIL-101(Cr) before and after loading PEI

Samples	Particle size ^[a] (nm)	SBET ^[b] ($\text{m}^2\cdot\text{g}^{-1}$)	Pore Volume ^[c] ($\text{cm}^3\cdot\text{g}^{-1}$)
A	~ 150	3149.69	1.71
B	~ 250	3354.93	1.89
B-PEI-300	-	495.23	0.35
A-PEI-300	-	33.46	0.13
A-PEI-1800	-	396.43	0.29
A-PEI-10000	-	457.17	0.24

[a] Particle size is estimated from the SEM images. [b] The specific surface area is calculated in the P/P_0 range of 0.05–0.2. [c] Values at $P/P_0=0.99$.

The N_2 adsorption/desorption isotherms of MIL-101(Cr) and PEI-loaded samples are measured at 77 K to evaluate their porosity. As shown in Figure S5, N_2 uptakes of MIL-101(Cr) are decreased dramatically after loading PEI. A-PEI-300 displays the lowest N_2 uptakes because the linear PEI is most effectively loaded into the inner pores in small MIL-101(Cr) crystals, which significantly impedes the N_2 adsorption. In contrast, B-PEI-300 displays much higher N_2 uptakes, indicating that the MOF particle size indeed plays an important role in loading PEI and thus the adsorption capacity. In large MIL-101(Cr) crystals, PEI is not sufficiently loaded into the inner pores and instead some PEI is still remained on the MOF surface. The corresponding BET surface area and pore volume for the samples are calculated from the isotherms and summarized in Table 1. Clearly, the surface area and pore volume of PEI-loaded samples are

increased with PEI molecular-weight increasing, albeit the loading conditions and amount are same. As shown in Figure S6, we have calculated the pore size distribution of samples based on Barrett-Joyner-Halenda method. In particular, the surface area and pore volume of A-PEI-300 are only $33.46\text{ m}^2\cdot\text{g}^{-1}$ and $0.13\text{ cm}^3\cdot\text{g}^{-1}$, respectively, which indicates that the framework pores of A are almost completely filled by PEI-300. The results are well consistent with the XRD characterizations.

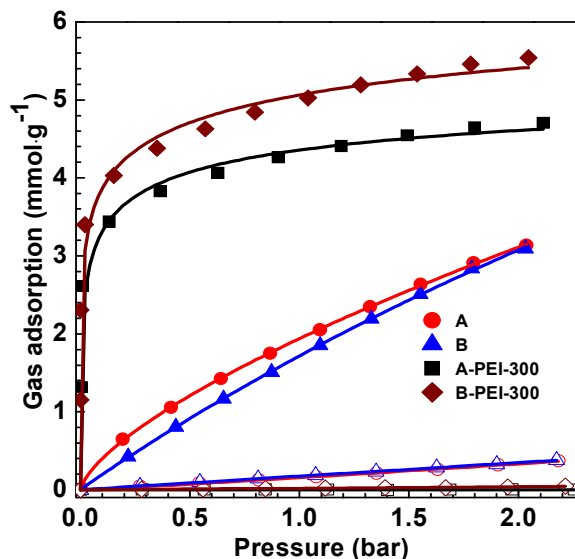


Figure 3. CO_2 (Filled) and N_2 (Hollow) adsorption isotherms of A, B, A-PEI-300 and B-PEI-300 at 25 °C. Lines are the fitted isotherms.

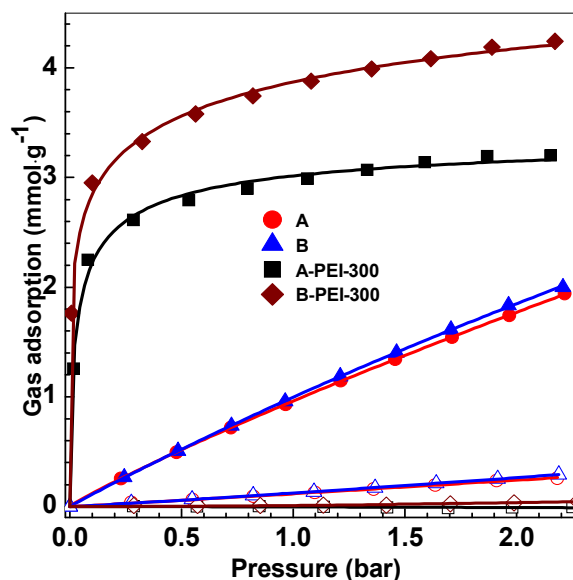


Figure 4. CO_2 (Filled) and N_2 (Hollow) adsorption isotherms of A, B, A-PEI-300 and B-PEI-300 at 50 °C. Lines are the fitted isotherms.

CO_2 and N_2 adsorption

We first start from the strategy of shrinking the MOF particle size. CO_2 and N_2 adsorption properties of all samples are measured at 25 °C and 50 °C, respectively. As shown in Figures 3 and 4, MIL-101(Cr) with small particle size displays slightly higher CO_2 adsorption capacity than large ones, albeit it has smaller surface area. It is probably attributed to more defects in

the small MIL-101(Cr) particles, which is caused by the more additives (e.g., CH_3COOLi) added in the synthesis solution.

The PEI-loaded samples display much higher CO_2 uptakes than the original MIL-101(Cr) (A and B) at low pressure and ambient temperature, whereas the N_2 uptakes are significantly decreased. This should be ascribed to the modified pore properties (e.g., pore size and polarity) of the MIL-101 (Cr) by loaded PEI that could interact strongly with CO_2 via the amine groups. Note that the pore volume of B-PEI-300 is nearly three times larger than that of A-PEI-300. However, the CO_2 adsorption capacity of the two composites only differ by 20%-40%. Apparently, the CO_2 adsorption capacity in these PEI/MOF composites is closely determined by the amount of amine groups available instead of the pore volume or surface area. In small MOF particles (sample A), more PEI can be loaded into the inner pores. However, CO_2 cannot diffuse deep into the pores to bind with them, probably because of the steric effect. Correspondingly, the strategy to shrink the MOF particle size fails to further improve the CO_2 adsorption capacity of the resulting composites. Fortunately, we will show in the next section that the small-size MOF particles are advantageous for the CO_2/N_2 selectivity.

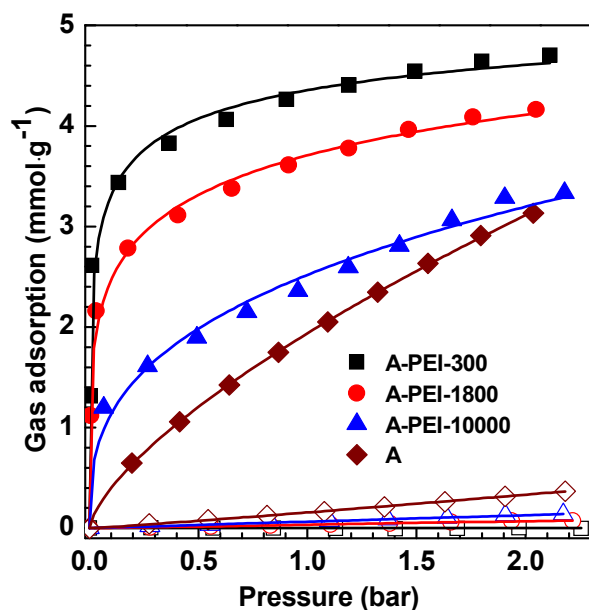


Figure 5. CO_2 (Filled) and N_2 (Hollow) adsorption isotherms of MIL-101(Cr) before and after loading PEI at 25°C. Lines are the fitted isotherms.

As aforementioned, the CO_2 uptake at around 0.15 bar is particularly important since the flue gas usually contains ~15% CO_2 .³⁵ At 0.15 bar and 25 °C, the A-PEI-300 and B-PEI-300 composites exhibit remarkable CO_2 adsorption uptakes of 3.6 $\text{mmol}\cdot\text{g}^{-1}$ and 4.1 $\text{mmol}\cdot\text{g}^{-1}$, respectively, whereas the CO_2 uptakes of A and B are only 0.52 $\text{mmol}\cdot\text{g}^{-1}$ and 0.29 $\text{mmol}\cdot\text{g}^{-1}$. The adsorption capacity of the as-prepared B-PEI-300 (4.1 $\text{mmol}\cdot\text{g}^{-1}$) is also higher than the commercially used amine-based (30 wt%) solutions (1.32 $\text{mmol}\cdot\text{g}^{-1}$) at 25 °C and 0.15 bar.⁴³ Furthermore, it is found that the CO_2 adsorption uptakes of PEI/MIL-101(Cr) composites increase very rapidly at the

pressure below 0.15 bar, which make them very attractive for industrial CO_2 capture. On the other hand, N_2 adsorption on A-PEI-300 cannot be even detected at 25 °C and 50 °C, whereas B-PEI-300 still exhibit some N_2 adsorption. This is consistent with their surface area and pore volumes. Indeed, for N_2 adsorption, the surface area and pore volumes play the most important role because the driving force is the weak van der Waals interactions.

We next investigate the strategy of applying larger molecular-weight PEI with more primary amine groups. As shown in Figure 5, the CO_2 adsorption capacity is clearly decreased with the PEI molecular-weight increasing, albeit the primary amine groups are expected to bind CO_2 more firmly than secondary groups. In contrast, the N_2 uptakes are increased with the PEI molecular-weight increasing. This is understandable because PEI with large molecular-weight has some branched chain, which greatly increases the diffusion resistance when it penetrates into MIL-101(Cr). Thus, PEI with large molecular-weight cannot be well-dispersed into the MIL-101(Cr) pores and instead some PEI would cover the MIL-101(Cr) crystal surface. The results are consistent with XRD, SEM and BET characterizations.

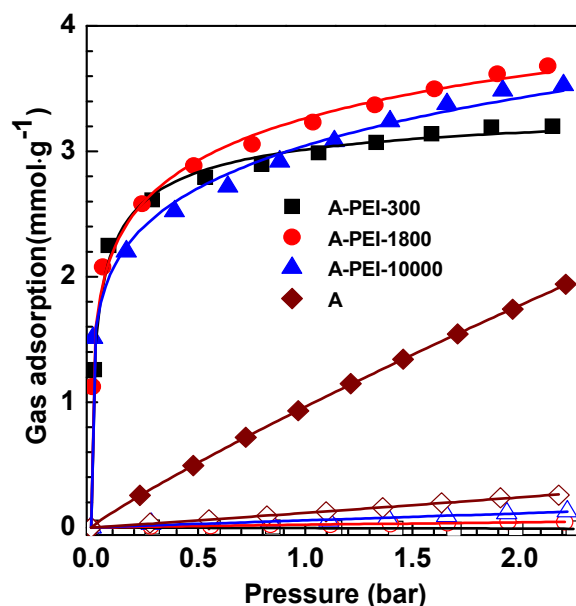


Figure 6. CO_2 (Filled) and N_2 (Hollow) adsorption isotherms of MIL-101(Cr) before and after loading PEI at 50 °C. Lines are the fitted isotherms.

Nevertheless, it does not suggest that high molecular-weight PEI is not suitable to fabricate PEI/MOF composites for CO_2 capture. As shown in Figure 6, the CO_2 adsorption capacity of A-PEI-10000 at 50 °C turns out to be higher than at 25 °C. Moreover, both A-PEI-1800 and PEI-10000 exhibit comparable and even higher CO_2 uptakes than A-PEI-300. The aforementioned SEM images clearly show that some unloaded PEI-10000 covers the MIL-101(Cr) particle surface, which may impede CO_2 from accessing the inner channels of the MIL-101(Cr) and blocks CO_2 adsorption. However, the modified pores and aggregated PEI that are not accessible to CO_2 molecules at low temperatures would become accessible at elevated temperatures due to the high elasticity of PEI. Furthermore, the high kinetic barrier for the diffusion of CO_2 from the surface into the filled pores would be overcome by the intense thermal motion

at higher temperature. On the contrary, large amount of PEI-300 with high elasticity loaded into the channels would expand at elevated temperature, which may further block the CO₂ diffusion channels and reduce the adsorption sites available for CO₂.

In addition, we should emphasize that most adsorbed CO₂ (>97%) can be desorbed from all samples at 100 °C under vacuum for 1 hour, as shown in Figure S7. That is, the present PEI/MOF materials should be used in temperature swing adsorption. The presence of water vapor does not decrease the CO₂ adsorption capacity of the adsorbent (Figure S8). The CO₂ adsorption kinetics shows that large amounts of CO₂ molecules can be rapidly adsorbed on the samples within a few minutes (Figure S9- S16). Note that, the CO₂ adsorption of A-PEI-300 become slower when the testing temperature is increased (50 °C), whereas the A-PEI-10000 sample displays higher CO₂ adsorption kinetics. The reason is probably similar for the change of their CO₂ adsorption capacity at high temperature, which has been discussed above.

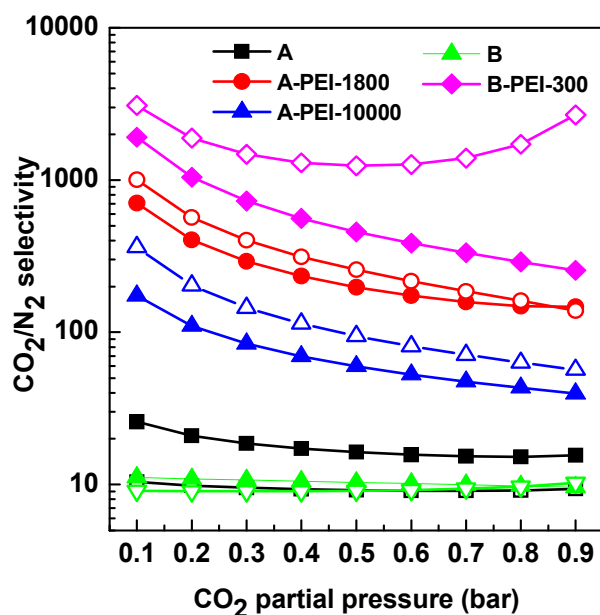


Figure 7. The selectivity of A, B, B-PEI-300, A-PEI-1800 and A-PEI-10000 for the CO₂ and N₂ mixture at a total pressure of 1 bar and temperatures of 25 °C (Filled) and 50 °C (Hollow), respectively.

We further calculated the amine efficiency of the PEI/MIL-101(Cr) composites. It was known that two active amines can hold one CO₂ molecule so that the theoretical maximum amine efficiency is 0.5.⁴⁴ However, extraordinary amine efficiency of up to 0.88 is achieved for the PEI/MIL-101(Cr) composites (see Table S1). Very recently, Long and coworkers reported a new mechanism for the CO₂ adsorption on the amines⁴⁵, suggesting that two amines can capture two CO₂ molecules simultaneously. Therefore, the theoretical maximum amine efficiency will be 1.0. We believe our experimental results clearly corroborate their reported mechanism.

We also measured the cyclic life of the three samples. Between each measurement, the sample was evacuated for 2 hours at 110 °C. The results show that the CO₂ capacity for A-PEI-300 is well retained (Figures S17 and S18). However, in the cases of the high molecular-weight PEI loaded sample, a slightly decreased CO₂

capacity is observed after several cycles (Figures S19 and S20), which is probably due to the decomposition of high molecular-weight PEI in the evacuation process.

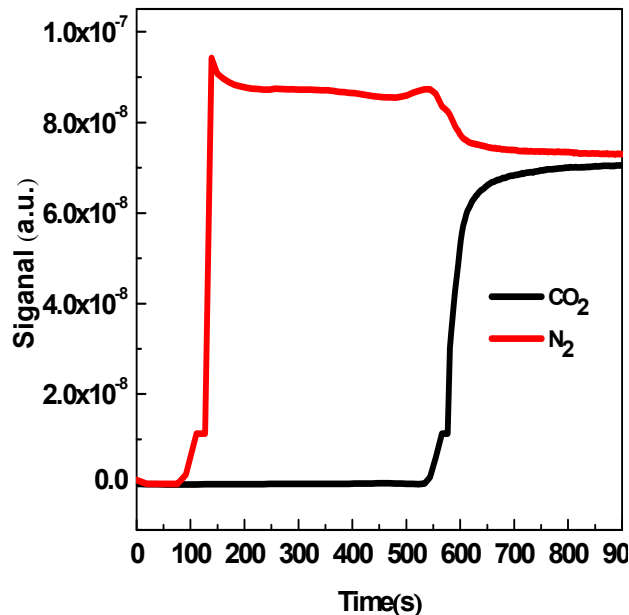


Figure 8. Breakthrough curves of B-PEI-300 with an equimolar CO₂/N₂ mixture at 25 °C

45 Selectivity of CO₂ over N₂

The separation performance as a function of CO₂ partial pressures for three samples is calculated. As shown in Figure 7, PEI-incorporated MIL-101(Cr) samples clearly show the dramatically enhanced CO₂/N₂ selectivity at tested temperatures. The CO₂/N₂ selectivities for A-PEI-1800 and A-PEI-10000 reach 1003 and 362 at a partial pressure of 0.1 bar and 50 °C, respectively. Compared to the poor CO₂/N₂ selectivity (~10) of original MIL-101(Cr), the selectivities of two composites are increased by 9930% and 3520%. Surprisingly, no N₂ adsorbed on A-PEI-300 can be detected at both 25 °C and 50 °C (Figure S21 and S22). As a result, the CO₂/N₂ selectivity of A-PEI-300 should be ultrahigh. This is because the inner pores is nearly filled with PEI-300 owing to the linear structure of PEI-300 and small particle size of sample A.

That is, the N₂ diffusion and adsorption channels are blocked. As for CO₂, they can still access the inner pores due to the smaller dynamic diameter. In addition, the strong interaction between PEI and CO₂ increases the possibility of CO₂ diffusion into the inner channels. In this manner, the PEI/MIL-101(Cr) samples can still maintain fairly good CO₂ adsorption ability at elevated temperature. However, N₂ adsorption is significantly decreased due to the weak van der Waals interactions. Accordingly, higher CO₂/N₂ selectivity of the PEI/MIL-101(Cr) composites can be observed at elevated temperatures. The excellent separation performance of PEI/MIL-101(Cr) composites for CO₂/N₂ mixture is corroborated by a breakthrough experiment performed at 25 °C. As shown in Figure 8, N₂ elutes rapidly from the column, whereas CO₂ only starts to elute after a period of time.

Conclusions

In conclusion, we have evaluated the selective CO₂ capture ability of a series of PEI/MIL-101(Cr) composites. All samples exhibit dramatically enhanced selective CO₂ adsorption capacity compared to the original MIL-101(Cr) at low pressure and ambient temperature. Shrinking the MOF particle size can facilitate the loading of PEI into the inner pores, yielding reduced surface area and pore volume. Thus, the resulting PEI/MIL-101(Cr) composites possess relatively lower CO₂ adsorption capacity, but higher selectivity of CO₂ over N₂. On the other hand, the molecular-weight of PEI also plays an important role. Lower molecular-weight PEI could readily diffuse into the inner pores, while larger PEI can be only partly loaded into the pores and the rest would be remained on the MOF surface. As a result, the as-prepared A-PEI-300 shows an excellent CO₂ adsorption capacity and ultrahigh CO₂/N₂ selectivity. At higher temperature (50 °C), the higher molecular-weight PEI/MIL-101(Cr) composites exhibit higher CO₂ adsorption capacity because of larger amount of primary amine groups.

Overall, polyamine/MOF composites are very promising candidate adsorbents for CO₂ capture from flue gas using the adsorption-driven technique. The energy cost for re-generation of polyamine/MOF adsorbent could be lower than amine-based solutions because the specific heat capacity of MOFs (around 1 J.g⁻¹.°C⁻¹) is much lower than aqueous solution (around 4.2 J.g⁻¹.°C⁻¹).⁴⁶ Nevertheless, the various parameters such as the molecular-weight and structures of polyamine, the porosity and particle size of MOF, must be carefully optimized to achieve the best selective CO₂ capture performance.

Acknowledgements

We acknowledge the financial support from national science foundation of China (51272260, 11104287), the aided program for science and technology innovative research team of Ningbo municipality (2011B82005), Ningbo NSF (2012A610117, 2012A610099) and major science and technology projects in Zhejiang Province (2012C12017-5).

Notes and references

a Ningbo Institute of Materials Technology and Engineering
Chinese Academy of Sciences

40 Ningbo Zhejiang 315201 (P.R. China)
E-mail: kongchl@nimte.ac.cn; chenliang@nimte.ac.cn

b School of Energy and power Engineering
University of Shanghai for Science and Technology
Shanghai 200093 (P.R. China)

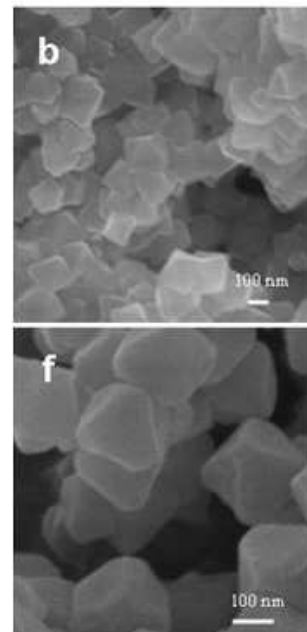
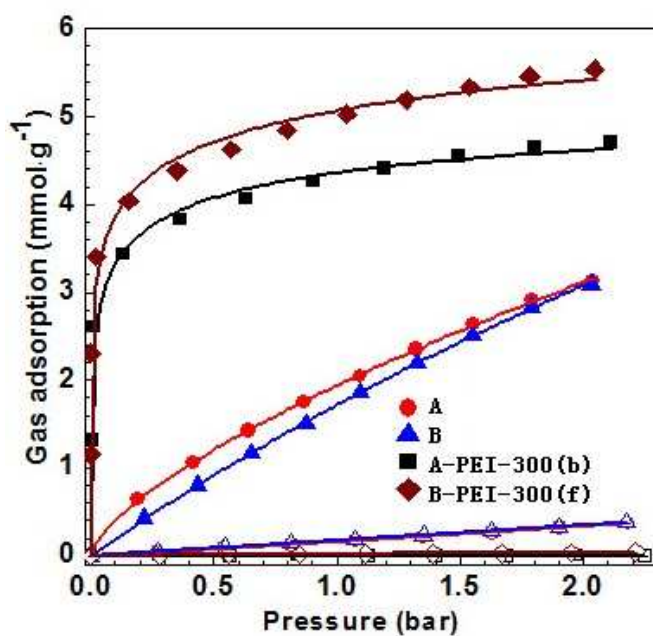
45 † Electronic Supplementary Information (ESI) available. See DOI: 10.1039/b000000x/

‡ Footnotes should appear here. These might include comments relevant to but not central to the matter under discussion, limited experimental and spectral data, and crystallographic data.

- 1 D. M. D'Alessandro, B. Smit, J. R. Long, *Angew. Chem. Int. Edit.* 2010, **122**, 6194–6219.
- 2 X. L. Ma, X. X. Wang, C. S. Song, *J. Am. Chem. Soc.* 2009, **131**, 5777–5783.
- 3 Carbon Dioxide Capture from Existing Coal Fired Power Stations; Revision Nov 2007; DOE/NETL 401/110907; National Energy Technology Laboratory, 2007.
- 4 A. Goepfert, M. Czaun, R. B. May, G. K. S. Prakash, G. A. Olah, S. R. Narayanan, *J. Am. Chem. Soc.* 2011, **133**, 20164–20167.

- 5 Y. Kuwahara, D. Y. Kang, J. R. Copeland, N. A. Brunelli, S. A. Didas, P. Bollini, C. Sievers, T. Kamegawa, H. Yamashita, C. W. Jones, *J. Am. Chem. Soc.* 2012, **134**, 10757–10760.
- 6 Y. Belmabkhout, R. Serna-Guerrero, A. Sayari, *Adsorption* 2011, **17**, 395–401.
- 7 A. Sayari, Y. Belmabkhout, R. Serna-Guerrero, *Chem. Eng. J.* 2011, **171**, 760–764.
- 8 A. Sayari, Y. Belmabkhout, *J. Am. Chem. Soc.* 2010, **132**, 6312–6314.
- 9 A. Heydari-Gorji, Y. Belmabkhout, A. Sayari, *Langmuir* 2011, **27**, 12411–12416.
- 10 S. Choi, J. H. Drese, P. M. Eisenberger, C. W. Jones, *Environ. Sci. Technol.* 2011, **45**, 2420–2427.
- 11 W. Chaikittisilp, J. D. Lunn, D. F. Shantz, C. W. Jones, *Chem.-Eur. J.* 2011, **17**, 10556–10561.
- 12 N. R. Stuckert, R. T. Yang, *Environ. Sci. Technol.* 2011, **45**, 10257–10264.
- 13 J. A. Wurzbacher, C. Gebald, A. Steinfeld, *Energy Environ. Sci.* 2011, **4**, 3584–3592.
- 14 L. B. Sun, J. R. Li, J. Park, H. C. Zhou, *J. Am. Chem. Soc.* 2012, **134**, 126–129.
- 15 X. Deng, S. Grunder, K. E. Cordova, C. Valente, H. Furukawa, M. Hmadeh, F. Gandara, A. C. Whalley, Z. Liu, S. Asahina, H. Kazumori, M. O'Keeffe, O. Terasaki, J. F. Stoddart, O. M. Yaghi, *Science* 2012, **336**, 1018–1023.
- 16 G. Ferey, C. Mellot-Draznieks, C. Serre, F. Millange, J. Dutour, S. Surble, I. Margiolaki, *Science* 2005, **309**, 2040–2042.
- 17 K. S. Park, Z. Ni, A. P. Cote, J. Y. Choi, R. D. Huang, F. J. Uribe-Romo, H. K. Chae, M. O'Keeffe, O. M. Yaghi, *Proc. Natl. Acad. Sci.* 2006, **103**, 10186–10191.
- 18 K. Sumida, M. L. Foo, S. Horike, J. R. Long, *Eur. J. Inorg. Chem.* 2010, **24**, 3739–3744.
- 19 Q. Yan, Y. Lin, P. Wu, L. Zhao, L. Cao, L. Peng, C. Kong, L. Chen, *ChemPlusChem* 2013, **78**, 86–91.
- 20 H. Furukawa, N. Ko, Y. B. Go, N. Aratani, S. B. Choi, E. Choi, A. O. Yazaydin, R. Q. Snurr, M. O'Keeffe, J. Kim, O. M. Yaghi, *Science* 2010, **329**, 424–428.
- 21 K. L. Kauffman, J. T. Culp, A. J. Allen, L. Espinal, W. Wong-Ng, T. D. Brown, A. Goodman, M. P. Bernardo, R. J. Pancoast, D. Chirdon, C. Matranga, *Angew. Chem. Int. Edit.* 2011, **50**, 10888–10892.
- 22 Y. Y. Liu, Z. Y. U. Wang, H. C. Zhou, *Greenh Gases* 2012, **2**, 239–259.
- 23 P. L. Llewellyn, S. Bourrelly, C. Serre, A. Vimont, M. Daturi, L. Hamon, G. De Weireld, J. S. Chang, D. Y. Hong, Y. K. Hwang, S. H. Jung, G. Ferey, *Langmuir* 2008, **24**, 7245–7250.
- 24 P. Nugent, Y. Belmabkhout, S. D. Burd, A. J. Cairns, R. Luebke, K. Forrest, T. Pham, S. Ma, B. Space, L. Wojtas, M. Eddaoudi, M. J. Zaworotko, *Nature* 2013, **494**, 80–84.
- 25 S. R. Caskey, A. G. Wong-Foy, A. J. Matzger, *J. Am. Chem. Soc.* 2008, **130**, 10870–10871.
- 26 Y. Lin, C. Kong, L. Chen, *RSC Adv.* 2012, **2**, 6417–6419.
- 27 S. N. Brune, D. R. Bobbitt, *Anal. Chem.* 1992, **64**, 166–170.
- 28 S. Couck, J. F. Denayer, G. V. Baron, T. Rémy, J. Gascon, F. Kapteijn, *J. Am. Chem. Soc.* 2009, **131**, 6326–6327.
- 29 B. Arstad, H. Fjellvåg, K. O. Kongshaug, O. Swang, R. Blom, *Adsorption* 2008, **14**, 755–762.
- 30 Y. Lin, Q. J. Yan, C. Kong, L. Chen, *Sci. Rep.* 2013, **3**, 1859–1866.
- 31 T. M. McDonald, W. R. Lee, J. A. Mason, B. M. Wiers, C. S. Hong, J. R. Long, *J. Am. Chem. Soc.* 2012, **134**, 7056–7065.
- 32 Q. Yan, Y. Lin, C. Kong, L. Chen, *Chem. Commun.* 2013, **49**, 6873–6875.
- 33 G. G. Qi, Y. B. Wang, L. Estevez, X. N. Duan, N. Anako, A. H. A. Park, W. Li, C. W. Jones, E. P. Giannelis, *Energy Environ. Sci.* 2011, **4**, 444–452.
- 34 A. Sayari, Y. Belmabkhout, E. Da'an, *Langmuir* 2012, **28**, 4241–4247.
- 35 E. J. Granite, H. W. Pennline, *Ind. Eng. Chem. Res.* 2002, **41**, 5470–5476.
- 36 R. Sips, *J. Chem. Phys.* 1948, **16**, 490–495.
- 37 J. An, N. L. Rosi, *J. Am. Chem. Soc.* 2010, **132**, 5578–5579.
- 38 R. Sips, *J. Chem. Phys.* 1950, **18**, 1024–1026.

-
- 39 T. M. McDonald, D. M. D'Alessandro, R. Krishna, J. R. Long, *Chem. Sci.* 2011, **2**, 2022–2028.
- 40 T. Loiseau, C. Serre, C. Huguenard, G. Fink, F. Taulelle, M. Henry, T. Bataille, G. Ferey, *Chem. Eur. J.* 2004, **10**, 1373–1382.
- 5 41 K. Sumida, D. L. Rogow, J. A. Mason, T. M. McDonald, E. D. Bloch, Z. R. Herm, T. H. Bae, J. R. Long, *Chem. Rev.* 2012, **112**, 724–781.
- 42 X. C. Xu, C. S. Song, J. M. Andresen, B. G. Miller, A. W. Scaroni, *Micropor. Mesopor. Mater.* 2003, **62**, 29–45.
- 10 43 A. N. M. Peeters, A. P. C. Faaij, W. C. Turkenburg, *Int. J. Greenh. Gas. Con.* 2007, **1**, 396–417.
- 44 W. Chaikittisilp, H-J. Kim, C. W. Jones, *Energy Fuels* 2011, **25**, 5528–5537.
- 45 N. Planas, A. L. Dzubak, R. Poloni, L-C. Lin, A. McManus, T. M. McDonald, J. B. Neaton, J. R. Long, B. Smit, L. Gagliardi, *J. Am. Chem. Soc.* 2013, **135**, 7402–7405.
- 15 46 B. Mu, K. S. Walton, *J. Phys. Chem. C.* 2011, **115**, 22748–22754.



Polyamine/MIL-101(Cr) composites exhibits excellent CO₂ capture ability at 0.15 bar and low temperatures.